Supplementary Information:

Solar-assisted co-electrolysis of glycerol and water for concurrent production of formic acid and hydrogen

Zunjian Ke,[a,b] Nicholas Williams,[b] Xingxu Yan,[c] Sabrina Younan,[b] Dong He,[a] Xianyin Song,[e] Xiaoqing Pan,[c,d] Xiangheng Xiao*[a] and and Jing Gu*[b]

[a]*Department of Physics, Key Laboratory of Artificial Micro- and Nano-structures of Ministry of Education, Wuhan University, Wuhan 430072, Hubei, China. E-mail: xxh@whu.edu.cn*

[b]*Department of Chemistry and Biochemistry, San Diego State University, San Diego, California 92182-1030, United States. E-mail: jgu@sdsu.edu*

[c]*Department of Materials Science and Engineering, University of California, Irvine, Irvine, California 92697, United States.*

[d]*Department of Physics and Astronomy, University of California, Irvine, Irvine, California 92697, United States.*

[e]*College of Materials Science and Engineering, Hunan University, Changsha 410082, Hunan, China.*

Supplementary Figures and Tables: Figure S1-Figure S23

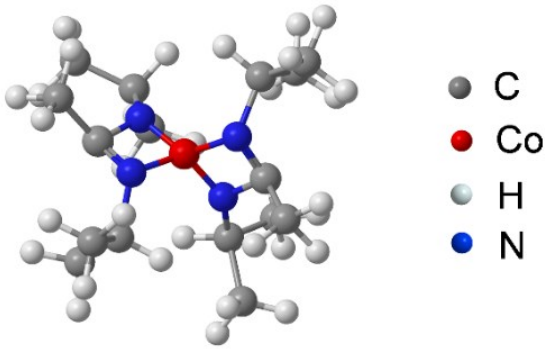

Supplementary Fig. S1. Molecular structure of Bis (N, N'-di-i-propylacetamidinato) cobalt (II) ($C_{16}H_{34}CoN_4$).

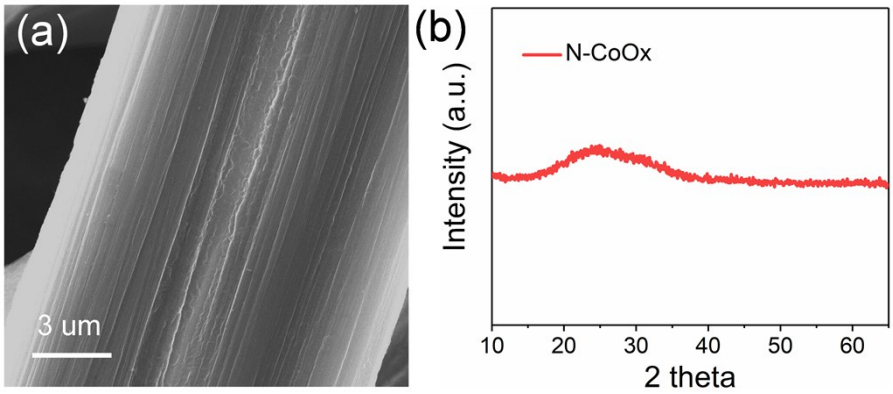

Supplementary Fig. S2. (a) SEM image and (b) XRD pattern of N-CoO_x.

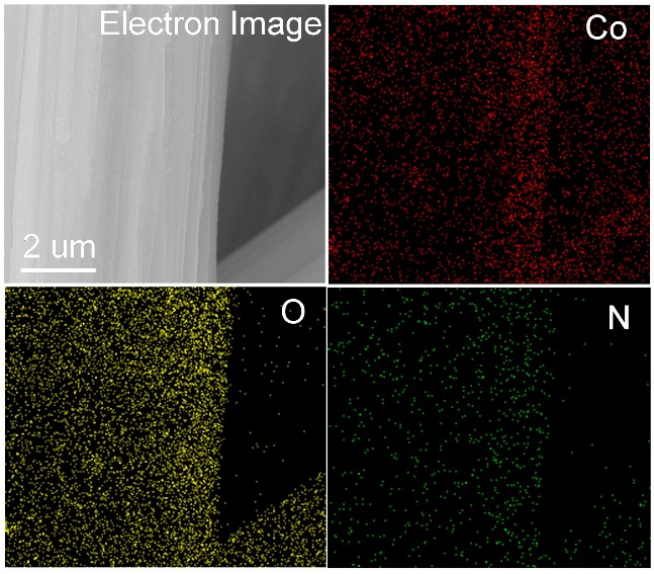

Supplementary Fig. S3. SEM-EDX elemental mappings of N-CoO_x on carbon fiber paper.

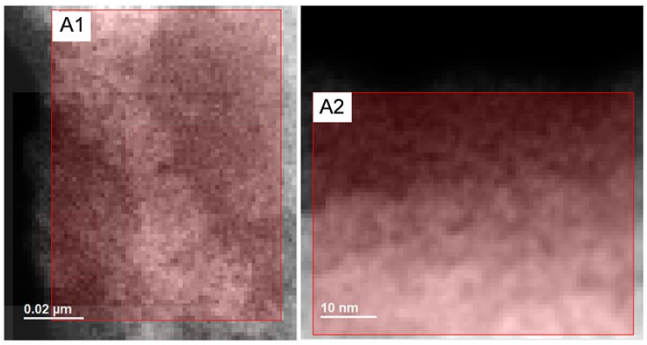

Element	Composition (at.%)	Composition (wt.%)
	A1	
C	38.2	24.2
N	12	8.9
O	38.7	32.6
Co	11.1	34.3
	A2	
C	39.8	24.7
N	10.6	7.6
O	37.5	31
Co	12.1	36.7

Supplementary Fig. S4. Elemental quantification analysis of N-CoO_x by STEM-EDS.

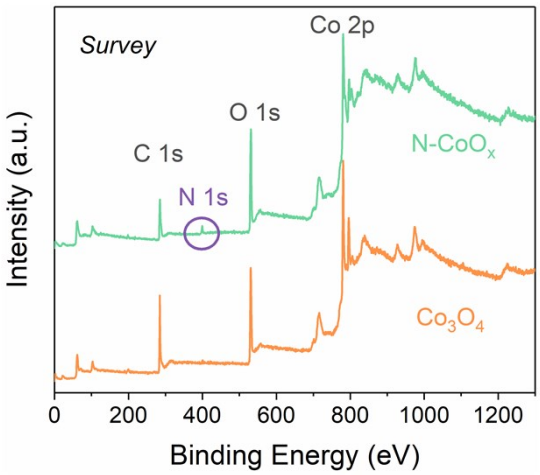

Supplementary Fig. S5. XPS survey of N-CoO_x and Co_3O_4.

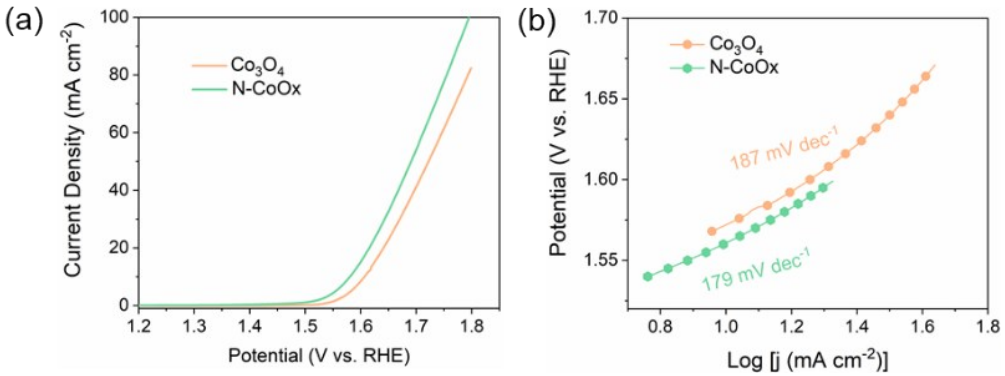

Supplementary Fig. S6. OER performances of Co_3O_4 and N-CoO_x in 1.0 M KOH solution. (a) LSV plots with 5 mV/s scan rate and without I-R compensation. (b) Tafel slopes calculated from (a).

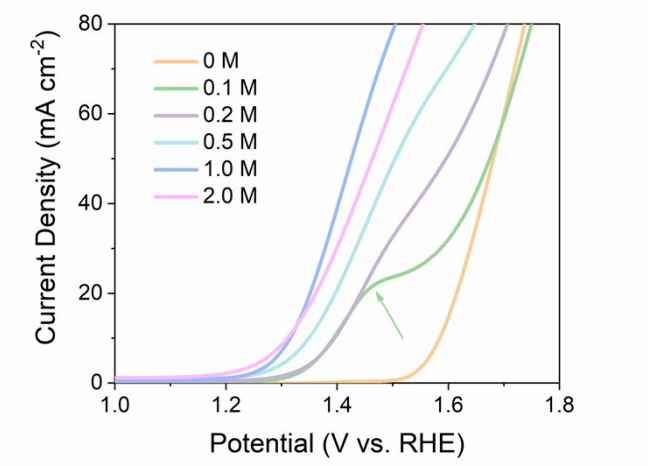

Supplementary Fig. S7. Glycerol oxidation in 1.0 M KOH solution with various concentrations of glycerol. (The turning point from glycerol oxidation to OER was pointed by green arrow. The performance tends to saturated as glycerol concentration increases.)

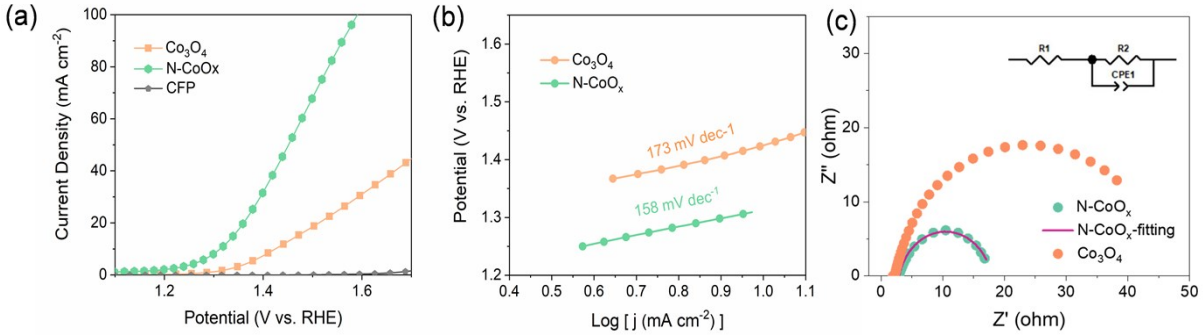

Supplementary Fig. S8. Glycerol oxidation performance of N-CoO_x and Co_3O_4. (a) LSV plots (5 mV/s), (b) Tafel slopes, and (c) EIS collected in 1.0 M KOH solution with 1.0 M glycerol (1.20 V vs. RHE) and the corresponding fitted curves and equivalent circuits. The related fitting parameters are shown in Table S3. The fitted result matched well with experimental data, indicating the rationality of the model and reliability of the conclusion.

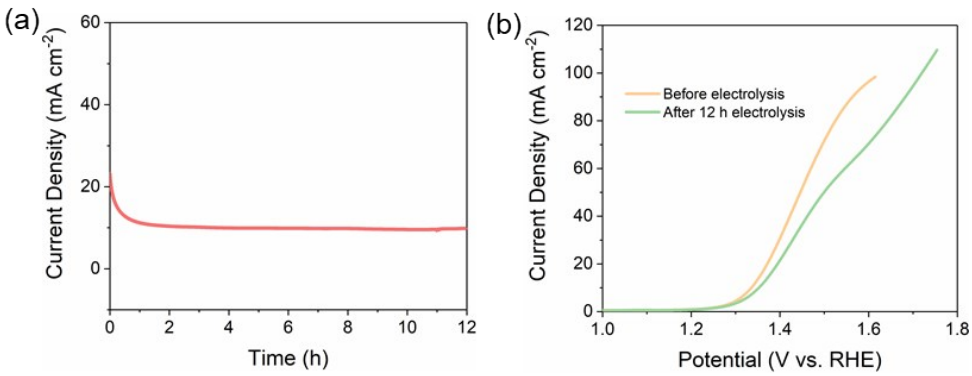

Supplementary Fig. S9. Long-term electrolysis measurements for glycerol electrooxidation. (a) I-t curve of 12 h electrolysis at 1.35V vs. RHE. (b) LSV plots before and after 12 h electrolysis.

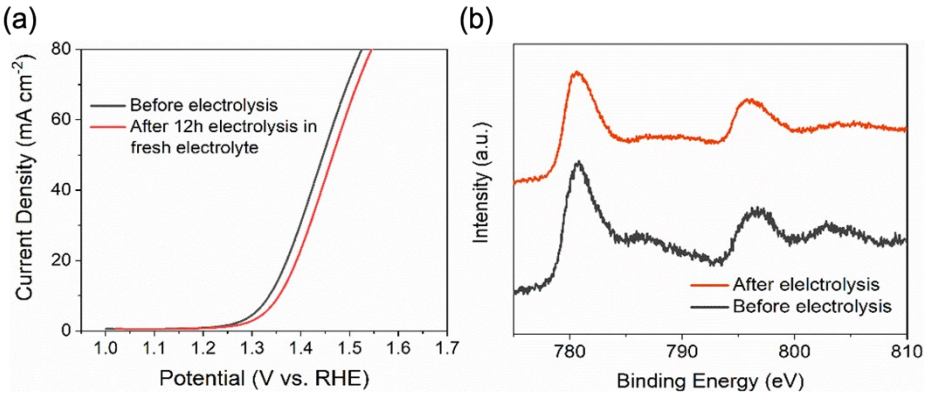

Supplementary Fig. S10. Comparison of N-CoO_x catalytic activity before and after 12-hour electrolysis. (a) LSV of CoOx prior to and post electrolysis (b) XPS of Co 2p prior to and post electrolysis.

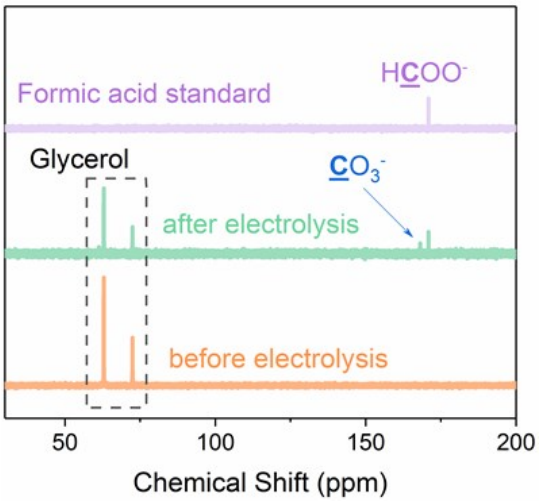

Supplementary Fig. S11. ^{13}C NMR of 1.0 M KOH solution with 1.0 M glycerol before and after 60-hour electrolysis at 1.35 V (RHE). (HCOOH standard concentration: 60 mM in 1.0 M KOH solution)

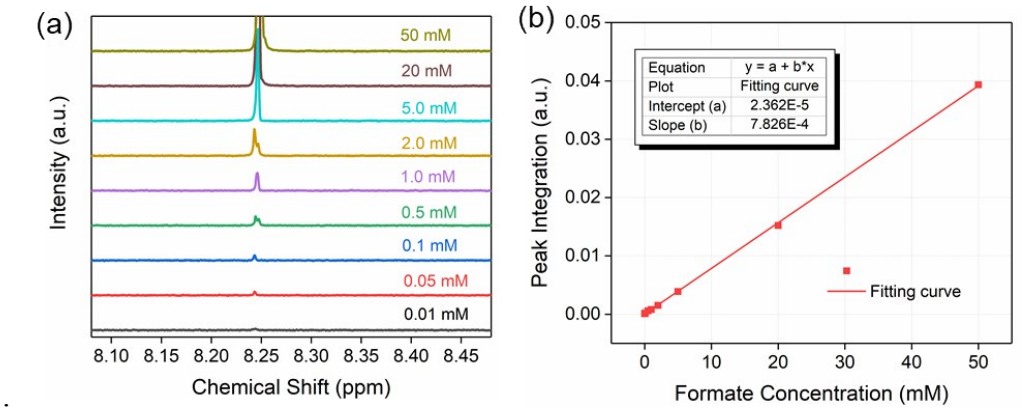

Supplementary Fig. S12. Formic acid concentration calibration. (a) ^{1}H NMR of 1.0M KOH solutions with various concentrations of formic acid. (b) Fitted formic acid concentration plot.

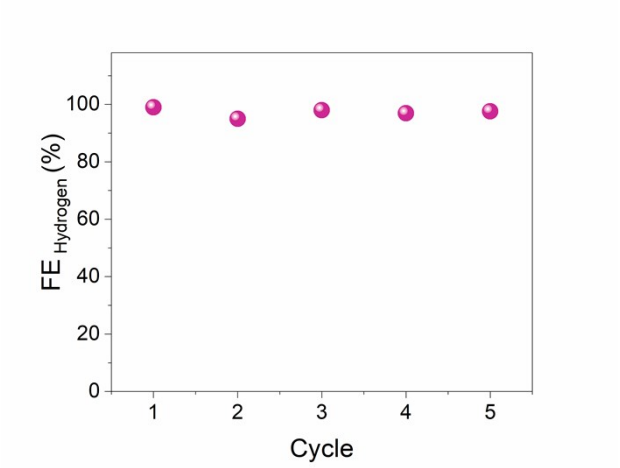

Supplementary Fig. S13. The FE of H_2 during co-electrolysis of glycerol and water. The electrolysis was performed at 1.35 V vs. RHE in the same three-electrode system. Each electrolysis cycle lasted 3 hours. The H_2 was detected by high-performance gas chromatography (GC).

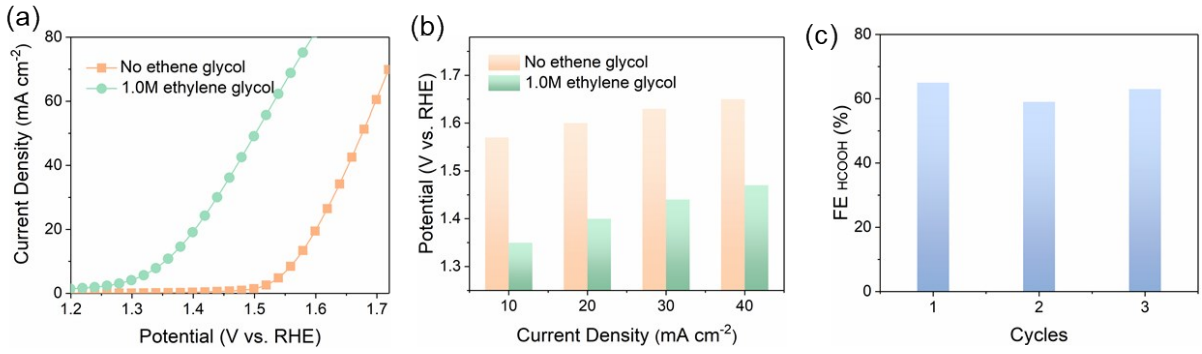

Supplementary Fig. S14. Ethylene glycol oxidation. (a) LSV plots (5 mV/s, without I-R compensation) and (b) potentials at different current density are collected in 1.0 M KOH solutions with and without 1.0 M ethylene glycol. (c) Faradaic efficiencies of formic acid for three successive electrolysis cycles at 1.40 V vs RHE.

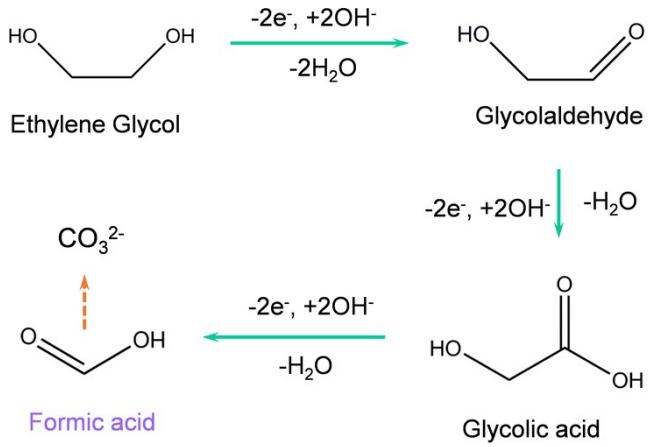

Supplementary Fig. S15. Proposed reaction pathway for ethylene glycol oxidation. The green solid and yellow dash arrow represent major and minor reaction routes, respectively. The formic acid was the major product (marked in purple). All steps were electrochemical oxidation processes with related electron transfer.

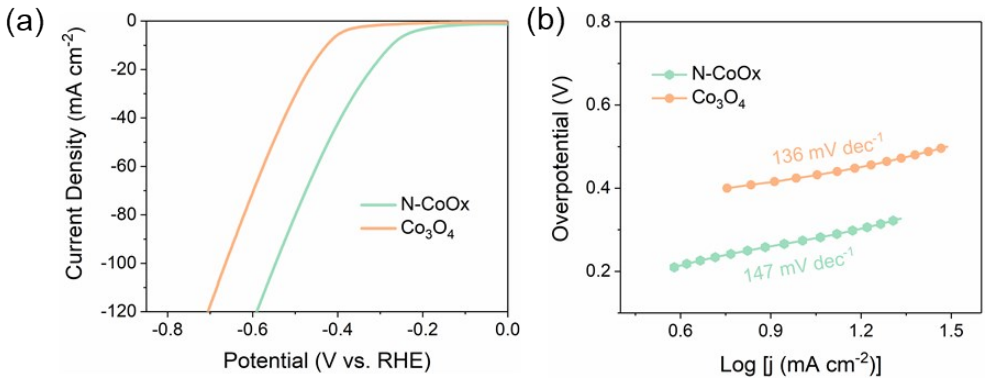

Supplementary Fig. S16. HER performance of Co3O4 and N-CoO_x in 1.0 M KOH solution. (a) LSV plots (5 mV/s). (b) Tafel slopes calculated from (a).

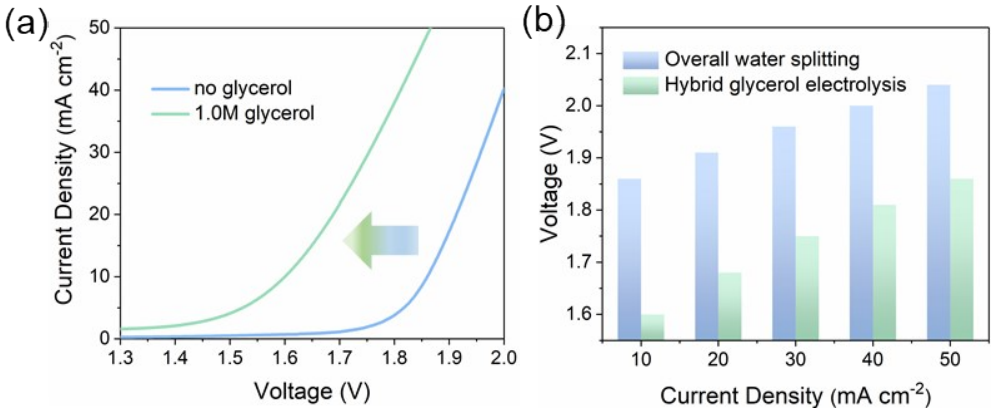

Supplementary Fig. S17. Hybrid glycerol electrolysis in coupled N-CoO_x||N-CoO_x system. (a) LSV plots of N-CoO_x in 1.0 M KOH solution with and without 1.0 M glycerol. (b) Cell voltages at various current densities.

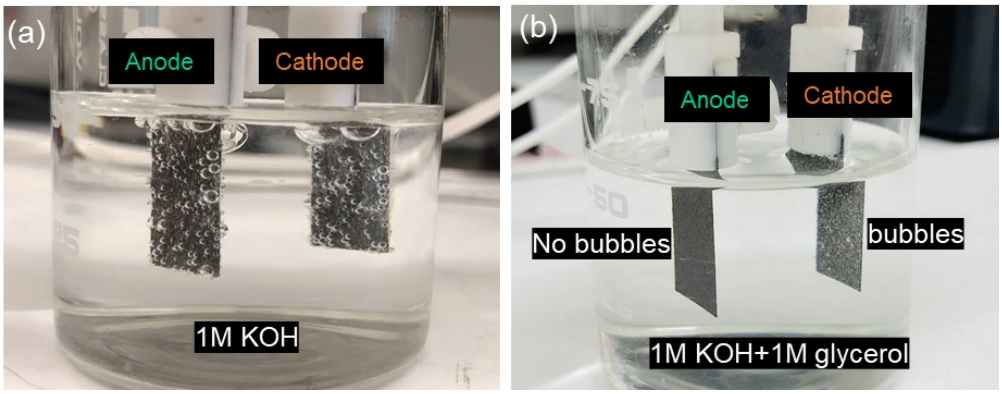

Supplementary Fig. S18. Digital pictures of N-CoOx|| N-CoOx hybrid system in (a) 1.0 M KOH solution and (b) 1.0 M KOH solution with 1.0 M glycerol.

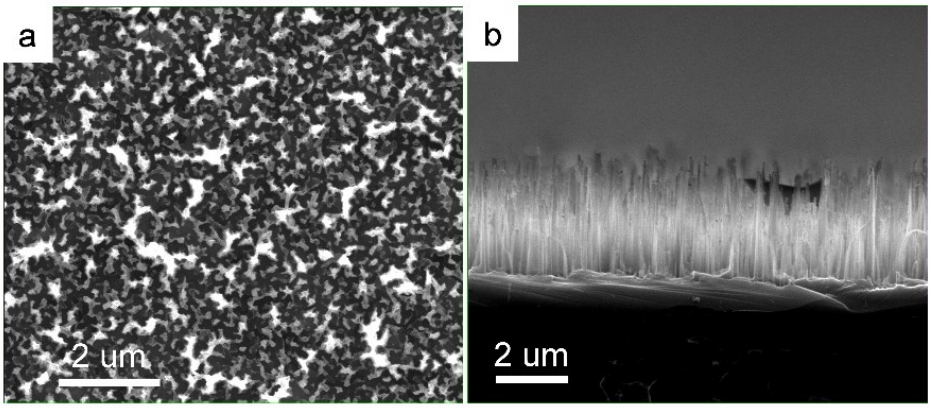

Supplementary Fig. S19. SEM images of Si NW-Pt. (a) Top view, (b) Cross-sectional view.

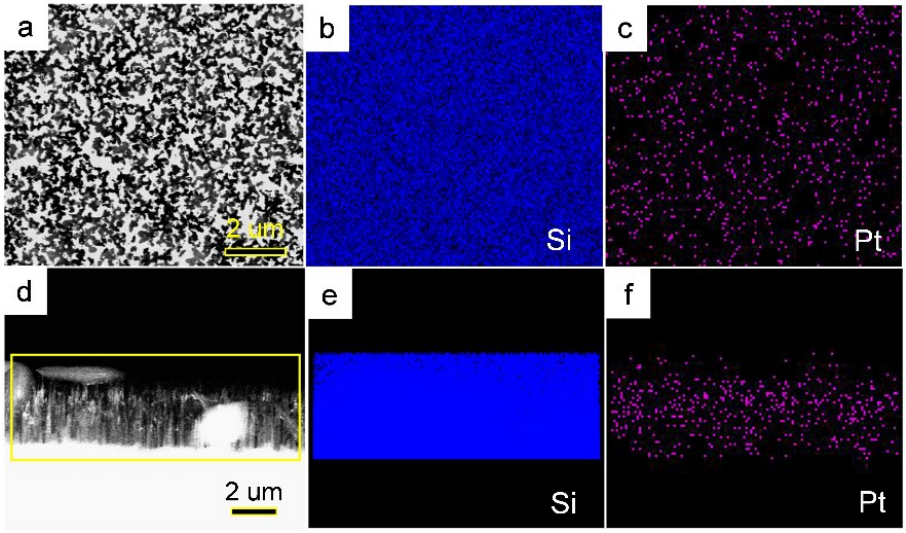

Supplementary Fig. S20. SEM-EDX elemental mapping for Si NW-Pt. (a-c) Top view, (d-f) Cross-sectional view.

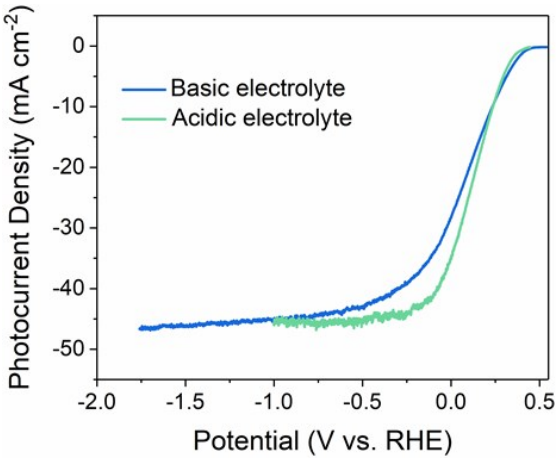

Supplementary Fig. S21. Photocurrent density of Si NW/Pt photoelectrode for hydrogen evolution in 1.0 M KOH and 0.5 M H_2SO_4 solution under AM 1.5G simulated sunlight illumination.

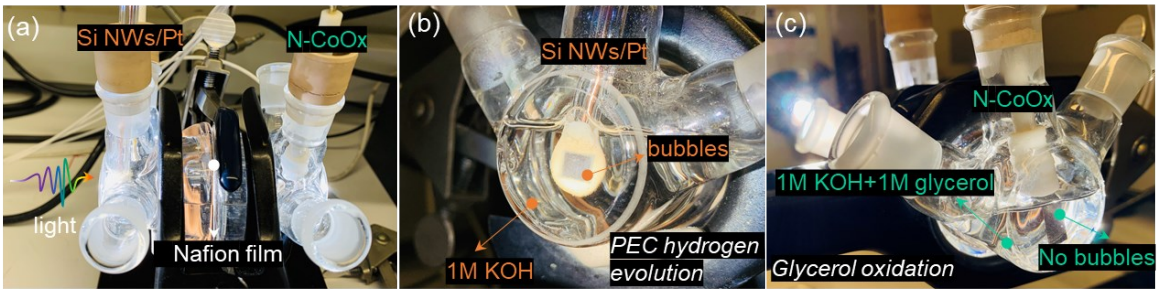

Supplementary Fig. S22. Digital pictures of N-CoO_x||Si NW/Pt hybrid system. (a) Front view, (b) left side view, and (c) right side view of the system.

Supplementary Table S1. Economic value evaluations for typical electrolysis and co-electrolysis of glycerol and water.

System	Overall reaction	products	Mass of anode products *vs.* per kg H_2 (kg)	Unit price of anode products (US $)	Total Values of anode products vs. per kg H_2 (US $)
Typical water electrolysis	$2H_2O=2H_2+O_2$	O_2 (anode) H_2 (cathode)	8	~ 0.10	~ 0.80
Co-electrolysis of glycerol and water	$C_3H_8O_3+3H_2O=3HCOOH+4H_2$	HCOOH (anode) H_2 (cathode)	17.25	1.0	17.25

Supplementary Table 2. Recent works for hybrid hydrogen evolution and organic oxidation.

catalyst	Electrolyte	Anodic major product	Faradaic efficiency	Three-electrode system			Two-electrode system		Ref
				E_{HER} (V)	E_{OER} (V)	E_{COR} (V)	E_1 (V)	E_2 (V)	
N-CoO_x anode Si NW-Pt photocathode	1 M KOH+1 M glycerol	Formic acid	96.2 %	+0.24 (photocathode)	1.58	1.31	1.34	**1.15**	**This work**
Ni-Mo-N/CFC anode Ni-Mo-N/CFC cathode	1 M KOH+0.1 M glycerol	Formic acid	95%	-0.043	1.57	1.30	1.62	1.36	1
$NiFeO_x$ anode $NiFeN_x$ cathode	1 M KOH+0.1 M glucose	Glucaric acid	87%	-0.0406	1.3 at 2.61 mA cm^{-2}	1.3 at 87.6 mA cm^{-2}	-	1.39 at100 mA cm^{-2}	2
$CuCo_2O_4$ anode	0.1 M KOH+0.1 M glycerol	Formic acid	89.1%	-	1.55-1.6	1.26	-	-	3
Ni_2P/Ni/NF anode Ni_2P/Ni/NF cathode	1M KOH +30mM Furfural	Furoic acid	Almost 100 %	-	1.55 (onset)	1.43 (onset)	1.59	1.48	4
CoNi-PHNs anode CoS_2-MoS_2 cathode	1 M KOH+1 M ethanol	acetic acid	99%	-	>1.7	1.39	~ 1.8	~1.6	5
Co-P-Cu foam anode Co-P-Cu foam cathode	1M KOH+50 mM 5-hydroxymethylfurfural	2,5-furandicarboxylic acid	~90%	-	1.53 (20 mA cm^{-2})	1.38 (20 mA cm^{-2})	1.59 (20 mA cm^{-2})	1.44 (20 mA cm^{-2})	6
NF/NiMoO-Ar anode NF/NiMoO-H_2 cathode	1 M KOH +0.5 M urea	N_2	-	11	-	1.37	1.55	1.38	7
NC@$CuCo_2N_x$/CF anode NC@$CuCo_2N_x$/CF cathode	1.0 M KOH+ 15 Mm benzyl alcohol	benzaldehydes	98%	105	1.46	1.25	1.62	1.55	8

Note: All the potentials here are V vs. RHE. All the potentials corresponded to 10 mA cm^{-2} unless otherwise marked. E_{COR}: potentials for chemical oxidation. E_1: cell voltages for overall water-splitting. E_2: cell voltages for the organic oxidation integrated HER.

Supplementary Table S3. The related EIS fitting parameters for N-CoO_x sample.

R1	R2	CPE1-T	CPE1-P
2.974	14.95	0.012041	0.85933

Supplementary References

1. Y. Li, X. Wei, L. Chen, J. Shi and M. He, *Nat. Commun.,* 2019, **10**, 1-12.
2. W. J. Liu, Z. Xu, D. Zhao, X. Q. Pan, H. C. Li, X. Hu, Z. Y. Fan, W. K. Wang, G. H. Zhao, S. Jin, G. W. Huber and H. Q. Yu, *Nat. Commun.*, 2020, **11**, 265.
3. X. Han, H. Sheng, C. Yu, T. W. Walker, G. W. Huber, J. Qiu and S. Jin, *ACS Catal.*, 2020, **10**, 6741-6752.

4. N. Jiang, X. Liu, J. Dong, B. You, X. Liu and Y. Sun, *ChemNanoMat*, 2017, **3**, 491-495.

5. W. Wang, Y. B. Zhu, Q. Wen, Y. Wang, J. Xia, C. Li, M. W. Chen, Y. Liu, H. Li, H. A. Wu and T. Zhai, *Adv. Mater.*, 2019, **31**, e1900528.

6. N. Jiang, B. You, R. Boonstra, I. M. Terrero Rodriguez and Y. Sun, *ACS Energy Lett.*, 2016, **1**, 386-390.

7. Z.-Y. Yu, C.-C. Lang, M.-R. Gao, Y. Chen, Q.-Q. Fu, Y. Duan and S.-H. Yu, *Energ. & Environ. Sci.*, 2018, **11**, 1890-1897.

8. J. Zheng, X. Chen, X. Zhong, S. Li, T. Liu, G. Zhuang, X. Li, S. Deng, D. Mei and J.-G. Wang, *Adv. Funct. Mater.*, 2017, **27**, 1704169.